JCI The Journal of Clinical Investigation

Activation of Gs signaling in mouse enteroendocrine K-cells greatly improves obesity- and diabetes-related metabolic deficits

Antwi-Boasiako Oteng, … , Frank Reimann, Jürgen Wess

J Clin Invest. 2024. https://doi.org/10.1172/JCI182325.

Research In-Press Preview **Endocrinology**

Graphical abstract

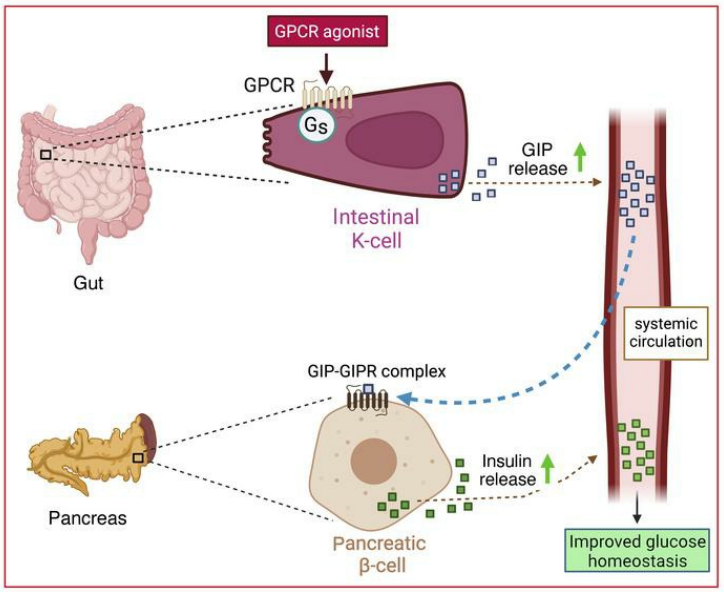

Activation of G_s signaling in mouse enteroendocrine K-cells greatly improves obesity- and diabetes-related metabolic deficits

Antwi-Boasiako Oteng*[1,2], Liu Liu[1], Yinghong Cui[1], Oksana Gavrilova[3], Huiyan Lu[4], Min Chen[5], Lee S. Weinstein[5], Jonathan E. Campbell[6], Jo E. Lewis[7], Fiona M. Gribble[7], Frank Reimann[7], Jürgen Wess[1,*]

[1]Molecular Signaling Section, Laboratory of Bioorganic Chemistry, National Institute of Diabetes and Digestive and Kidney Diseases, Bethesda, Maryland, USA.

[2]Center for Research on Genomics and Global Health (CRGGH), National Human Genome Research Institute (NHGRI), National Institutes of Health (NIH), Bethesda, Maryland, USA.

[3]Mouse Metabolism Core, National Institute of Diabetes and Digestive and Kidney Diseases, Bethesda, Maryland, USA.

[4]Mouse Transgenic Core Facility, National Institute of Diabetes and Digestive and Kidney Diseases, Bethesda, MD 20892, USA.

[5]Signal Transduction Section, Metabolic Diseases Branch, National Institute of Diabetes and Digestive and Kidney Diseases, Bethesda, Maryland, USA.

[6]Duke Molecular Physiology Institute, Duke University, Durham, North Carolina, USA.

[7]MRC Metabolic Diseases Unit, Institute of Metabolic Science, University of Cambridge, Addenbrooke's Hospital, Cambridge, United Kingdom.

Address correspondence to:

Dr. Jürgen Wess

Laboratory of Bioorganic Chemistry

Molecular Signaling Section, National Institute of Diabetes and Digestive and Kidney Diseases

Bldg. 8A, Room B1A-05, 8 Center Drive

Bethesda, Maryland 20892, USA

Tel: 301-402-3589; Email: jurgenw@niddk.nih.gov

or

Dr. Antwi-Boasiako Oteng

Laboratory of Bioorganic Chemistry

Molecular Signaling Section, National Institute of Diabetes and Digestive and Kidney Diseases

Bldg. 8A, Room B1A-05, 8 Center Drive

Bethesda, Maryland 20892, USA

Tel: 301-827-5417; Email: antwi.oteng@nih.gov

Conflict of interest: The authors have declared that no conflict of interest exists.

Running title: G_s signaling in enteroendocrine K-cells

Abstract

Following a meal, glucagon-like peptide-1 (GLP1) and glucose-dependent insulinotropic polypeptide (GIP), the two major incretins promoting insulin release, are secreted from specialized enteroendocrine cells (L- and K-cells, respectively). Although GIP is the dominant incretin in humans, the detailed molecular mechanisms governing its release remain to be explored. GIP secretion is regulated by the activity of G protein-coupled receptors (GPCRs) expressed by K-cells. GPCRs couple to one or more specific classes of heterotrimeric G proteins. In the present study, we focused on the potential metabolic roles of K-cell G_s. First, we generated a mouse model that allowed us to selectively stimulate K-cell G_s signaling. Second, we generated a mouse strain harboring an inactivating mutation of *Gnas*, the gene encoding the α-subunit of G_s, selectively in K-cells. Metabolic phenotyping studies showed that acute or chronic stimulation of K-cell G_s signaling greatly improved impaired glucose homeostasis in obese mice and in a mouse model of type 2 diabetes, due to enhanced GIP secretion. In contrast, K-cell-specific *Gnas* knockout mice displayed markedly reduced plasma GIP levels. These data strongly suggest that strategies aimed at enhancing K-cell G_s signaling may prove useful for the treatment of diabetes and related metabolic diseases.

Introduction

Incretins are polypeptide hormones that are released from specialized enteroendocrine cells after the intake of food (1-4). Numerous studies have shown that these intestinal peptide hormones play key roles in the maintenance of proper glucose homeostasis and various other important metabolic functions (1-4). The two major incretins are glucagon-like peptide 1 (GLP1) and glucose-dependent insulinotropic polypeptide (GIP) which act on pancreatic β-cells to promote the release of insulin, thus contributing to the restoration of euglycemia after a meal (1-4). Besides β-cells, both incretins can also modulate the activity of several other cell types, including specific neuronal subpopulations (4-6). The physiological actions of GLP1 and GIP are mediated by GLP1 and GIP receptors, respectively, which belong to the subfamily of class B G protein-coupled receptors (GPCRs) (7).

The recent development of highly selective GIP and GLP1 receptor antagonists has made it possible to study the relative contribution of endogenous GIP and GLP1 to enhanced insulin release and improved glucose homeostasis (3, 8). Studies with these agents have shown that the beneficial metabolic effects of GIP and GLP1 are additive, and that GIP is quantitatively more important than GLP1 in promoting insulin release and affecting postprandial glucose excursions, at least in healthy individuals (3, 8).

During the past decades, much research has focused on agents that can selectively stimulate GLP1 receptors for therapeutic purposes. These studies have led to the development of several clinically approved GLP1 receptor agonists that are highly efficacious in the treatment of type 2 diabetes (T2D) and obesity (9, 10). In contrast, research in the GIP field has been held back by initial findings that patients with T2D failed to release significant amounts of insulin following

exogenously administered GIP (reviewed in (11)). Moreover, studies with GIP and GIP receptor mutant mice and GIP receptor agonists and antagonists resulted in seemingly contradictory results (12, 13). Early work demonstrated that GIP receptor and GIP knockout mice showed reduced body weight gain under different experimental conditions, associated with improvements in glucose homeostasis (14, 15). The potential role of GIP receptor signaling to the regulation of body weight is also consistent with the outcome of a more recent human genome-wide association study (GWAS) (16). These findings stimulated efforts to develop GIP receptor blockers as appetite-suppressive and antidiabetic drugs (reviewed in (17)). On the other hand, more recent studies showed that GIP receptor agonists, particularly in combination with GLP1 receptor agonists, are highly efficacious in reducing body weight and improving glucose homeostasis (reviewed in (17)). For example, treatment with tirzepatide, an FDA-approved dual GIP/GLP1 receptor agonist, causes pronounced reductions in body weight and striking improvements in blood glucose control (18, 19). Clinical trials demonstrated that tirzepatide administration resulted in more robust weight loss and improved glycemic control as compared to treatment with GLP1 receptor agonists alone (18, 19). The cellular and molecular mechanisms underlying the observation that both activation and blockade of GIP receptors can lead to similar metabolic outcomes is currently the matter of intense investigation.

Højberg *et al.* (20) demonstrated that the insulinotropic activity of GIP can be restored in T2D, at least partially, after drug-induced lowering of blood glucose levels. Moreover, a recent study in which diabetic individuals were treated with a selective GIP receptor antagonist indicated that endogenous GIP retains considerable efficacy in promoting insulin release in T2D (21).

Prompted by these recent studies, we tested the hypothesis that strategies aimed at enhancing the release of endogenous GIP from K-cells might prove beneficial for the treatment of T2D and obesity-related metabolic disorders. Like other cell types, K-cells express numerous GPCRs that are linked to different functional classes of heterotrimeric G proteins ($G_{q/11}$, G_s, $G_{i/o}$, and $G_{12/13}$) (6, 22). As a general rule, a specific GPCR is expressed in multiple tissues and cell types (23). For this reason, it has not been possible to explore the in vivo metabolic consequences of selectively modulating GIP release from enteroendocrine K-cells by traditional pharmacological techniques. To overcome this obstacle, we took advantage of the availability of designer GPCR known as DREADDs (Designer Receptors Exclusively Activated by Designer Drugs) (24-27). Following the recent development of a G_{12}-coupled DREADD (28), DREADDs that are selectively linked to each of the four major G protein families are now available as powerful chemogenetic tools (27, 29). DREADDs can be selectively activated by synthetic drugs such as clozapine-N-oxide (CNO) (24) or deschloroclozapine (DCZ) (30, 31), which are otherwise pharmacologically inert, at least when used in the proper dose range (24, 27, 30).

In the present study, we examined whether selective activation of G_s signaling in mouse K-cells was able to promote GIP release in vivo and, if so, how G_s-mediated GIP secretion affected impaired glucose homeostasis in obese mice and in mice with partial ablation of β-cells mimicking human T2D. To address these questions, we generated a DREADD mouse strain that selectively expressed a G_s DREADD (GsD) (25) in mouse K-cells and subjected the resulting mutant mice to systematic metabolic studies. To complement this work, we also generated and analyzed another mouse model that lacked functional $G\alpha_s$ selectively in K-cells.

We found that chemogenetic activation of G_s signaling in K-cells led to greatly improved glucose homeostasis in obese, glucose-intolerant mice and in a mouse model of T2D, most likely

due to increased plasma GIP levels. In contrast, mice lacking functional $G\alpha_s$ selectively in K-cells showed reduced plasma GIP levels. Our data suggest that agents capable of promoting G_s signaling in K-cells (e.g. agonists acting on G_s-coupled receptors endogenously expressed by K-cells) may emerge as drugs useful for the treatment of T2D and related metabolic disorders.

Results

Generation and functional characterization of K-GsD mice.

To generate mutant mice that express the GsD designer receptor selectively in enteroendocrine K-cells (K-GsD mice), we crossed *ROSA26-LSL-Gs-DREADD-CRE-luc* mice (short name: LSL-GsD mice) (32) with *Gip-Cre* mice that express Cre-recombinase under the transcriptional control of the *Gip* promotor (33) (Figure 1A). LSL-GsD mice that lacked the *Gip-Cre* transgene served as control littermates. Since the GsD receptor carried an N-terminal hemagglutinin (HA) tag (32), we used an anti-HA antibody to detect the expression of GsD in mouse enteroendocrine cells. Immunofluorescence staining showed that GsD was only expressed by GIP-positive K-cells (Figure 1B). We found that ~67% of GIP-positive cells expressed the GsD designer receptor (18 out of total of 27 K-cells; note that K-cells are very rare; see Methods for details).

To explore whether activation of GsD receptors in K-cells affected endogenous GIP secretion, we carried out studies with male K-GsD mice and control littermates consuming regular chow. The two groups did not differ in body weight (Figure 1C). Prior to injection of DCZ, a highly selective DREADD agonist (34), plasma GIP levels were significantly higher in K-GsD mice, as compared to control littermates ($P = 0.000587$; Student's t-test) (Figure 1D). Previous studies demonstrated that the GsD DREADD can signal, to a variable degree, in a ligand-independent fashion in certain cell types (25, 32). For this reason, the slightly elevated plasma GIP levels found with K-GsD mice in the absence of DCZ are most likely due to constitutive signaling via K-cell GsD.

Strikingly, oral administration of a DCZ bolus (10 μg/kg) to K-GsD mice led to pronounced increases in plasma GIP levels 15 and 60 min after drug treatment (Figure 1D). DCZ

administration had no significant effect on plasma GIP levels in control mice (Figure 1D). The DCZ-induced increases in plasma GIP levels in K-GsD mice did not affect blood glucose (Figure 1E) and plasma insulin (Figure 1F) levels, consistent with previous observations that GIP promotes insulin release only at elevated glucose concentrations (6, 8, 35, 36) (also see the following paragraph). Moreover, plasma GLP1 levels remained unchanged after DCZ treatment of either K-GsD mice or control littermates (Figure 1G), consistent with the selective expression of GsD in K-cells.

In an additional experiment, we treated K-GsD mice and control littermates (males) orally with either glucose (2 g/kg) or DCZ (10 μg/kg) alone, or a glucose/DCZ mixture. We then monitored plasma GIP levels for up to 4 hours (Supplemental Figure 1). Treatment of control littermates with glucose alone caused a significant increase in plasma GIP levels over basal only at the 15 min time point (Supplemental Figure 1A). A similar pattern was observed with glucose-treated K-GsD mice (Supplemental Figure 1A). However, due to a certain degree of ligand-independent GsD signaling (see previous paragraph), plasma GIP levels were consistently higher in glucose-treated GsD mice, as compared to glucose-treated control littermates. As expected, treatment of control littermates with DCZ alone had no significant effect on plasma GIP levels (Supplemental Figure 1B). In contrast, DCZ-treated K-GsD mice displayed higher plasma GIP levels over basal at the 15 and 60 min time points. Again, due to constitutive signaling by GsD, plasma GIP levels were higher at all time points in DCZ-treated K-GsD mice, as compared to DCZ-treated control littermates (Supplemental Figure 1B). The temporal pattern of GIP release observed with K-GsD mice co-treated with glucose plus DCZ was similar to that observed with DCZ-treated K-GsD mice (Supplemental Figure 1C). However, absolute plasma GIP levels were markedly higher in the co-treated K-GsD mice (note the different labeling of the y axis in panel

1C). Taken together, these data suggest that GsD-mediated activation of G_s signaling in K-cells results in GIP responses that are similar in magnitude to that observed after glucose treatment. However, the GsD-mediated GIP response showed a longer duration of action. As expected, K-GsD mice co-treated with glucose plus DCZ showed more robust increases in plasma GIP levels, as compared to K-GsD mice treated with either glucose or DCZ alone.

Acute activation of K-cell G_s signaling improves glucose tolerance in mice consuming regular chow.

We next subjected K-GsD mice and control littermates (males) consuming regular chow to an oral glucose tolerance test (OGTT). Treatment of K-GsD and control mice with an oral glucose bolus alone resulted in comparable blood glucose excursions in the two groups of mice (Figure 2A). In contrast, following oral co-administration of glucose (2 g//kg) and DCZ (10 μg/kg), the K-GsD mice showed a striking improvement in glucose tolerance (Figure 2B), suggesting that this effect results from enhanced G_s signaling in K-cells. Insulin tolerance tests (0.75 U/kg, i.p.) indicated that K-GsD mice and control littermates showed similar peripheral insulin sensitivity, either in the absence or presence of DCZ (Figure 2C and 2D, respectively). We observed similar phenotypes when we carried out glucose and insulin tolerance tests with female K-GsD mice and control littermates (Supplemental Figure 2A-D).

To explore whether the improved glucose tolerance displayed by DCZ-treated K-GsD mice (Figure 1B) was mediated by elevated GIP levels, we measured plasma GIP and insulin levels 10 min after oral co-administration of glucose (2 g//kg) and DCZ (10 μg/kg). This treatment resulted in significantly higher plasma GIP and insulin levels in both K-GsD mice and control littermates (Figure 2E, F). However, these increases in plasma GIP and insulin levels were

clearly more pronounced in the K-GsD mice (Figure 2E, F). Oral co-administration of glucose and DCZ had no significant effect on plasma GLP1 levels in either of the two groups of mice (Figure 2G). This latter finding is not surprising since plasma GLP1 is rapidly degraded by the actions of dipeptidyl peptidase-4 and neprilysin after oral treatment of mice with glucose (33, 37).

To provide more direct evidence that the improved glucose tolerance displayed by K-GsD mice co-treated with glucose and DCZ resulted from enhanced GIP signaling, we injected K-GsD mice and control littermates with a monoclonal, antagonistic GIP receptor antibody (Gipg013; 20 mg/kg, s.c.) (38, 39). Forty-eight hours later, mice received an oral bolus of glucose plus DCZ, followed by the monitoring of blood glucose levels. Strikingly, administration of the GIP receptor antibody completely abolished the ability of DCZ to improve glucose tolerance in K-GsD mice (Figure 2H). These data indicate that activation of G_s signaling in intestinal K-cells improves glucose tolerance in a GIP-dependent manner.

Acute stimulation of K-cell G_s signaling greatly improved glucose tolerance in obese mice.
We next investigated whether acute activation of G_s signaling in K-cells was able to improve impaired glucose tolerance in diet-induced obese mice (males). Starting at 8 weeks of age, we maintained K-GsD mice and control littermates on a HFD for 8 weeks and then subjected the mice to a series of metabolic tests. After 14 weeks of HFD feeding, the two groups of mice showed similar body weight and body composition (lean and fat mass) (Figure 3A-C). Moreover, food intake did not differ significantly between obese K-GsD and control mice (Figure 3D).

Interestingly, obese K-GsD showed a striking improvement in glucose tolerance even in the absence of DCZ (Figure 3E), most likely due to the fact that the GsD receptor shows a certain

degree of ligand-independent signaling (25, 32). Moreover, oral co-treatment of obese K-GsD mice with glucose (1 g/kg) plus DCZ (10 μg/kg) resulted in an even more pronounced improvement in glucose tolerance (Figure 3F, G). To corroborate the concept that enhanced GIP signaling is responsible for the striking improvement in glucose tolerance observed with HFD K-GsD mice, we injected HFD K-GsD mice and HFD control littermates with a GIP receptor monoclonal antibody (20 mg/kg, s.c.; GIPg013) (38, 39). Forty-eight hours later, all mice received an oral bolus of glucose plus DCZ, followed by the measurement of blood glucose levels. We found that the pronounced improvement in glucose tolerance displayed by DCZ-treated HFD K-GsD mice was significantly attenuated after administration of the GIP receptor antibody (Figure 3H). As observed with chow-fed mice, HFD K-GsD mice and control littermates showed similar decreases in blood glucose levels in i.p. insulin tolerance tests, independent of the presence or absence of DCZ (Figure 3I-K).

To test the hypothesis that the greatly improved glucose tolerance displayed by HFD K-GsD mice resulted from enhanced GIP and insulin secretion, we measured plasma GIP and insulin levels after oral co-administration of glucose (1 g/kg) and DCZ (10 μg/kg). We found that both plasma GIP and insulin levels were significantly elevated in HFD K-GsD mice 5 min after co-treatment with glucose plus DCZ, as compared to HFD control littermates (Figure 3L, M). Plasma GLP1 levels remained unaffected in both groups of mice following co-administration of oral glucose plus DCZ (Figure 3N).

Taken together, these findings strongly suggest that selective activation of G_s signaling in K-cells stimulates the secretion of GIP and insulin when blood glucose levels are elevated, thus reversing the glucose intolerance characteristic of obese mice.

Chronic activation of K-cell G_s signaling improves glucose tolerance in obese mice.

We also explored whether chronic stimulation of G_s signaling in K-cells affected adiposity and adiposity-associated metabolic deficits in HFD K-GsD mice. To address this question, we put 12-week-old male K-GsD mice and control littermates on a HFD and added DCZ (10 mg/l) to the drinking water. We then monitored body weight gain over a 12-week period. Although body weight trended to be reduced in the K-GsD mice, this effect did not reach statistical significance (Figure 4A). Moreover, the two groups of mice did not differ in body composition (lean and fat mass; Figure 4B) and food intake (Figure 4C) measured 11 weeks after initiation of HFD feeding (Figure 4C).

After two weeks of HFD feeding, blood glucose levels were similar in K-GsD mice and control littermates maintained on DCZ water (Figure 4D). However, plasma GIP levels were significantly elevated in both groups of mice at this point, with K-GsD mice showing markedly higher GIP levels than control mice (Figure 4E). This observation suggests that GsD receptor-mediated GIP release was not subject to desensitization. HFD-induced increases in plasma insulin levels did not differ significantly between the two groups of mice (Figure 4F), consistent with previous observations that GIP-induced insulin release requires elevated blood glucose levels (35, 36). Moreover, plasma GLP1 levels were not affected in HFD K-GsD mice and control littermates under these experimental conditions (Figure 4G).

We next subjected K-GsD mice and control littermates maintained on the HFD and DCZ drinking water for 8 weeks to an OGTT. Strikingly, the K-GsD mice showed a marked improvement in glucose tolerance, as compared to the control mice (Figure 4H). Under these experimental conditions, the two groups of mice showed similar insulin tolerance (Figure 4I). To investigate the mechanism underlying the improved glucose tolerance displayed by the HFD K-

GsD mice maintained on DCZ water, we treated both groups of mice with an oral bolus of glucose (1 g/kg), followed by the monitoring of blood glucose, and plasma GIP, insulin, and GLP1 levels. Consistent with the OGTT data, HFD K-GsD mice showed significantly smaller increases in blood glucose levels than HFD control mice 30 min after administration of the glucose bolus (Figure 4J). Strikingly, HFD K-GsD mice showed a more robust increase in both plasma GIP and insulin levels 5 min after glucose treatment (Figure 4K, L). Plasma GLP1 levels remained unaltered under these experimental conditions (Figure 4M). The time course of the observed changes in blood glucose and plasma GIP and insulin levels strongly suggests that GsD-mediated increases in GIP release trigger enhanced insulin secretion which in turn lead to reduced glucose-induced hyperglycemic responses.

While HFD K-GsD mice consuming DCZ water showed greatly improved glucose tolerance in the OGTT (Figure 4H), this effect was not observed when HFD K-GsD mice and control littermates were subjected to an ipGTT (Figure 4N, O). In agreement with this observation, an i.p. glucose bolus (1 g/kg) did not lead to a rise in plasma GIP levels in both groups of mice (Figure 4P). However, due to the ligand-independent activity of the GsD receptor (25, 32), HFD K-GsD mice showed elevated plasma GIP levels at all time points (including 'time 0'), as compared to their HFD control littermates (Figure 4P).

Since GIP has been implicated in the regulation of energy homeostasis (reviewed in ref. (40)), we performed a series of indirect calorimetry studies at thermoneutrality (30ºC) and ambient temperature (22ºC). We found that HFD K-GsD mice consuming DCZ water did not differ from their control littermates in total energy expenditure, respiratory exchange ratio (RER), and total ambulatory activity at 30ºC or 22ºC (Supplemental Figure 3). In sum, these data indicate that chronic activation of G_s signaling in K-cells leads to enhanced circulating GIP levels

that promote euglycemia but have no effect on body weight, food intake, and energy expenditure.

Chronic activation of K-cell G_s signaling greatly reduced hyperglycemia in a mouse model of diabetes.

We next examined whether chronic activation of K-cell G_s signaling might improve glucose homeostasis in a mouse model of diabetes. Specifically, we treated K-GsD mice and control littermates (8-week-old males) with a relatively low dose of streptozotocin (STZ) for five consecutive days (50 mg/kg i.p. daily; (41, 42)). Previous studies demonstrated that this treatment protocol does not destroy all β-cells but reduces β-cell mass by ~80% (41, 42), thus mimicking the pronounced decrease in β-cell mass characteristic for advanced T2D (43). In agreement with this observation, a recent study demonstrated that β-cells from mice treated with multiple low doses of STZ show similar changes in gene expression as β-cells in human T2D (44).

All mice received DCZ via the drinking water (10 mg/l), starting from the first day of STZ treatment, except for WT control mice that received no treatment at all. Four weeks after the first STZ injection, both K-GsD mice and control littermates showed a ~75% reduction in islet size, as compared to WT mice treated with neither STZ nor DCZ (Figure 5A, B). Moreover, at this time point, pancreatic insulin and glucagon content did not differ significantly between STZ+DCZ-treated K-GsD mice and control littermates (Figure 5C, D). However, in comparison with WT mice that had not been treated with STZ+DCZ, pancreatic insulin content was significantly reduced, while pancreatic glucagon content was significantly increased (Figure 5C, D). Strikingly, while STZ+DCZ-treated control mice developed severe hyperglycemia during the

4-week observation period, this response was greatly reduced in STZ+DCZ-treated K-GsD mice (Figure 5E). The different groups of mice showed similar body weight throughout the 4-week observation period (Supplemental Figure 4).

Interestingly, STZ+DCZ-treated K-GsD mice showed significantly increased plasma GIP and insulin levels four weeks after the start of the experiment (Figure 5F and G, respectively), as compared to the STZ+DCZ-treated control littermates. Plasma levels of GLP1 and glucagon (Figure 5H, I) did not differ significantly between the different groups of mice. Taken together, these data indicate that chronic stimulation of K-cell G_s signaling potently counteracts the development of hyperglycemia in a mouse model of diabetes, most likely via GIP-mediated stimulation of insulin secretion.

We next explored the possibility that treatment of WT mice with mouse [D-Ala^2]GIP (42, 45), a relatively stable GIP analog (46, 47), could reduce STZ-induced hyperglycemia in a fashion similar to that observed with STZ+DCZ-treated K-GsD mice. In agreement with the outcome of a recent study (48), we found that i.p. treatment of WT mice for 4 weeks with [D-Ala^2]GIP ((24 nmoles/kg per dose; two injections per day; injection times: 9 am and 6 pm) had no significant effect on STZ-induced hyperglycemia (Supplemental Figure 5). Since previous studies have shown that endogenous GIP is rapidly metabolized to GIP (3-42) which can act as a weak partial agonist at GIP receptors (49), it is possible that GIP (3-42) contributes to the beneficial metabolic effects observed after G_s-mediated stimulation of GIP release in this STZ diabetes model.

Generation and metabolic characterization of K-Gs-KO mice.

We next investigated whether the lack of K-cell G_s signaling resulted in metabolic phenotypes that were opposite to those displayed by DCZ-treated K-GsD mice. To address this question, we generated mice that selectively lacked $G\alpha_s$ in intestinal K-cells (K-Gs-KO mice). To obtain this mouse strain, we crossed *Gnas*$^{flox/flox}$ mice (50) with *Gip-Cre* mice (33) (Figure 6A). The resulting *Gnas*$^{flox/+}$ *Gip-Cre* mice were then backcrossed to *Gnas*$^{flox/flox}$ mice to generate *Gnas*$^{flox/flox}$ *Gip-Cre* mice (K-Gs-KO mice) and control littermates (*Gnas*$^{flox/flox}$ mice). To study the efficiency of Cre-mediated inactivation of *Gnas*, we followed a previously published FACS protocol (51) to obtain K-cells from the mouse duodenum. As expected, duodenal K-cells prepared from K-Gs-KO mice showed a ~90% reduction in *Gnas* expression, as compared to non-K-cells present in the mouse duodenum (Figure 6B).

H&E staining studies showed that the lack of K-cell G_s had no obvious effect on the overall morphology of the proximal intestine (duodenum; Figure 6C). Moreover, K-Gs-KO mice and control littermates did not differ in body weight (Figure 6D), small intestine weight (Figure 6E), and intestinal content of GIP and GLP1 (Figure 6F, G). However, plasma GIP levels were significantly reduced (by ~50%) in the K-Gs-KO mice (Figure 6H). Plasma GLP1 levels did not differ significantly between K-Gs-KO mice and control littermates (Figure 6I). Food intake of singly housed mice remained unaffected by the lack of K-cell $G\alpha_s$ signaling (Figure 6J).

We next subjected K-Gs-KO mice and control littermates to a 24-hour fast, followed by a 2-hour re-feeding period (diet: regular chow). The two groups of mice showed no significant differences in body weight under these experimental conditions (Figure 6K). At the end of the 2-hour re-feeding period, the K-Gs-KO mice showed a modest but significant increase in blood glucose levels, as compared to their control littermates (Figure 6L). The plasma levels of non-

esterified fatty acids (NEFAs) did not differ between the two groups of mice, both in the fasted state and after the refeeding period (Figure 6M).

In control mice, plasma GIP levels were greatly increased at the end for the 2-hour re-feeding period (Figure 6N). In striking contrast, plasma GIP levels were not elevated in K-Gs-KO mice under these experimental conditions (Figure 6N), suggesting that the lack of G_s-stimulated GIP release is responsible for the greater increase in blood glucose levels observed with the K-Gs-KO mice after the refeeding period. In agreement with this notion, the increase in plasma insulin levels triggered by refeeding was significantly less pronounced in K-Gs-KO mice, as compared to their control littermates (Figure 6O). In the fasted state, plasma GLP1 levels were significantly increased in the absence of K-cell G_s signaling (Figure 6P). However, plasma GLP1 levels did not differ significantly between K-Gs-KO mice and control littermates after the 2-hour refeeding period (Figure 6P; see (37)). Plasma glucagon levels did not differ between the two groups of mice, either in the fasting state or after the refeeding period (Figure 6Q).

Inhibition of G_s signaling in K-cells reduces GIP secretion but does not affect glucose homeostasis in lean and diet-indued obese mice.

To study the effects of inactivating G_s signaling in K-cells on systemic glucose homeostasis, K-Gs-KO mice and control littermates consuming regular chow received an oral glucose bolus (2 g/kg). Ten min later, blood glucose levels were elevated to a similar degree in both groups of mice (Figure 7A). However, glucose-induced elevations in plasma GIP levels were reduced by ~50% in the K-Gs-KO mice (Figure 7B). Glucose-dependent increases in plasma insulin levels were comparable in magnitude between the two groups of mice (Figure 7C). Plasma GLP1 levels remained unchanged under these experimental conditions (Figure 7D).

Similarly, K-Gs-KO mice and control littermates maintained on regular chow showed similar blood glucose excursions in an OGTT (Figure 7E). Likewise, exogenously administered insulin (0.75 U/kg, i.p.) caused similar decreases in blood glucose levels in the two groups of mice (ITT; Figure 7F). We obtained similar results with female K-Gs-KO and control mice (reduced plasma GIP but unaltered plasma GLP1 and blood glucose excursions in OGTT and ITT assays) (Supplemental Figure 6A-D).

Since the ingestion of triglycerides strongly stimulates the release of GIP from K-cells (6, 52) , we next treated K-Gs-KO mice and control littermates with an oral bolus of olive oil (10 μl/g), followed by the measurement of blood glucose and plasma hormone and metabolite levels 60 min later. At this time point, blood glucose levels did not differ significantly between the two groups of mice (Figure 7G). In control mice, olive oil administration resulted in a very robust increase in plasma GIP levels (Figure 7H). Strikingly, this effect was greatly reduced in K-Gs-KO mice (Figure 7H). Treatment with olive oil had no significant effect on plasma insulin levels in both groups of mice under these experimental conditions (Figure 7I). However, in K-Gs-KO mice, olive oil administration caused a small but significant increase in plasma GLP1 levels (Figure 7J), perhaps resulting from the activation of a compensatory pathway caused by low circulating GIP levels (Figure 7H). Plasma levels of NEFAs were similar between the two groups of mice prior to and 60 min after olive oil administration (Figure 7K).

To investigate whether the lack of K-cell G_s signaling affected adiposity and adiposity-linked metabolic deficits in mice consuming a HFD, we subjected K-Gs-KO mice and control littermates that had been maintained on a HFD for 14 weeks to a series of metabolic tests. Under these experimental conditions, the two groups of mice did not differ significantly in body weight gain, body composition (lean versus fat mass), and daily food intake (Supplemental Figure 6E-

H). HFD K-Gs-KO and control littermates also showed comparable blood glucose excursions in OGTT and ITT assays (Supplemental Figure 6I, J). Moreover, following, an oral glucose bolus (1 g/kg), blood glucose (Supplemental Figure 6K) and plasma insulin levels (Supplemental Figure 6M) were elevated to a similar extent in the two groups of mice. However, glucose-stimulated GIP secretion was strongly reduced in the HFD K-Gs-KO mice 10 min after treatment with the oral glucose bolus (Supplemental Figure 6L), as observed with K-Gs-KO mice consuming regular chow (Figure 7B). Plasma GLP1 levels remained unchanged in the two groups under these experimental conditions (Supplemental Figure 6N).

Since the HFD K-Gs-KO mice did not display any detectable deficits in glucose homeostasis under different experimental conditions, we speculated that signaling via GLP1, the second major incretin, was able to compensate for impaired GIP release caused by the lack of K-cell G_s signaling. To test this hypothesis, we treated HFD K-Gs-KO and control littermates with an antagonistic GLP1 receptor antibody (19.2 mg/kg, s.c.; Glp10017) (38) or vehicle (PBS), followed by an OGTT. We found that administration of the GLP1 receptor antibody led to strikingly enhanced blood glucose excursions in both K-Gs-KO and control mice (Supplemental Figure 6O). However, the magnitude of this effect was similar in the two groups of mice in comparison with the PBS-treated mice. These observations suggest that the relatively low plasma GIP levels characteristic for K-Gs-KO mice under different experimental conditions suffice to maintain euglycemia. Taken together, these data indicate that inhibition of K-cell G_s signaling reduces GIP secretion but does not affect glucose tolerance in lean and obese mice.

The lack of K-cell G_s signaling does not affect the ability of a GPR40 agonist to stimulate GIP secretion.

A recent study demonstrated that agonist activation of a G_q-coupled DREADD selectively expressed in mouse K-cells leads to a pronounced increase in GIP secretion (53). Previous work has also shown that GPR40 (alternative name: FFAR1), a G_q-coupled receptor that is activated by long-chain fatty acids, is enriched in enteroendocrine K-cells (reviewed in (6)). To test the possibility that FFAR1 activity can promote GIP release in K-Gs-KO mice, we treated K-Gs-KO mice and control littermates with AM1638, a highly selective and efficacious FFAR1 agonist (54, 55). We found that oral AM1638 treatment (30 mg/kg (54)) of K-Gs-KO mice resulted in a robust increase in GIP secretion (Supplemental Figure 7). The magnitude of this response was not significantly different from that observed with control littermates (Supplemental Figure 7). Taken together these data suggest that receptor-activated G_q signaling in K-cells remains as a major stimulant of GIP secretion in K-Gs-KO mice.

G_s-coupled receptors endogenously expressed by K-cells.

To explore which endogenous G_s-coupled receptors are expressed by mouse and human K-cells, we mined previously published scRNAseq data (56, 57). The ten mouse and human G_s-coupled receptors that showed the highest expression levels are displayed in Supplemental Figure 8. In mouse K-cells, *Gpr119* was by far the most abundant G_s-coupled receptor (as far as gene expression levels are concerned). On the other hand, in human K-cells, *GPBAR1* was the predominant G_s-coupled receptor transcript. Among the receptors listed in Supplemental Figure 8, five G_s-coupled receptors are expressed in both mouse and human K-cells including the G protein-coupled bile acid receptor 1 (*GPBAR1*), the prostanoid EP4 receptor (*PTGER4*), the $VPAC_1$ receptor (*VIPR1*), the GIP receptor (*GIPR*), and the A_{2A} adenosine receptor (*ADORA2A*).

The G_s-coupled receptors expressed by human K-cells can be considered potential targets for drugs able to stimulate GIP secretion for therapeutic purposes.

Discussion

During the past decade, highly potent and efficacious GLP1/GIP receptor co-agonists (e.g. tirzepatide (58-60) have been developed for the treatment of T2D and obesity (61-63). Interestingly, a recent study demonstrated that the ability of tirzepatide to promote insulin release from human islets requires the presence of islet GIP receptors (64). These and other studies have generated renewed strong interest in exploring the physiological and pathophysiological roles of GIP. In the present study, we tested the hypothesis that selective stimulation of GIP release from enteroendocrine K-cells might be able to restore euglycemia in obese mice and in a mouse model of T2D (STZ-induced reduction in β-cell mass).

The GIP-producing K-cells, like other enteroendocrine cells, express dozens of GPCRs that are predicted to modulate GIP release (6, 57, 65). GPCRs represent very attractive therapeutic targets, primarily due to their cell surface localization and their ability to modulate the activity of many important cellular signaling pathways (66). Since the individual members of the GPCR superfamily are usually expressed by multiple tissues and cell types (23), it has not been possible to stimulate a specific GPCR or G protein signaling pathway in K-cells in vivo by using classical pharmacological techniques.

To overcome this obstacle, we decided to apply a chemogenetic approach involving the use of DREADD technology (26, 27, 29). Miedzybrodzka et al. (67) recently showed that treatment

of human duodenal organoids with forskolin, a potent activator of adenylyl cyclase, was able to strongly stimulate the release of GIP. Prompted by this observation, we decided to test the hypothesis that selective activation of G_s signaling (active $G\alpha_s$ is a potent stimulant of adenylyl cyclase) leads to enhanced GIP release in vivo. Specifically, we generated a mouse model that expressed a G_s DREADD (GsD) (25) selectively in K-cells (K-GsD mice) (Figures 1A, B).

In agreement with our hypothesis, acute treatment of either lean or obese K-GsD mice with DCZ, a highly selective DREADD agonist (34), led to marked increases in plasma GIP levels (Figures 1D, 2E, 3L). In the absence of co-administered glucose, these elevated GIP levels had no effect on insulin secretion and glucose homeostasis in general. This observation is consistent with previous findings that GIP triggers insulin secretion only when blood glucose levels are elevated (6, 8, 35, 36). In contrast, oral co-treatment of lean or obese K-GsD mice with DCZ plus glucose resulted in striking increases in plasma GIP and insulin levels and greatly improved glucose tolerance. Since the observed increases in plasma GIP and insulin levels preceded the beneficial effect on blood glucose levels (Figures 2E, 2F, 3L, 3M, 4K, and 4L), our data strongly support the concept that activation of K-cell G_s signaling stimulates the secretion of GIP which then acts on β-cell GIP receptors to promote the release of insulin, followed by the reduction of blood glucose levels and improved glucose homeostasis. The observation that stimulation of K-cell G_s signaling was able to restore euglycemia in obese, glucose-intolerant mice is of particular translational interest (Figure 3F).

In general, obesity is associated with marked increases in plasma GIP levels (12, 68, 69) (also see Figure 4E). Because of this finding, it is widely assumed that elevated GIP levels are linked to GIP receptor desensitization (reviewed in (12, 70)). However, our data clearly show that further increasing plasma GIP levels in obese mice leads to greatly improved glucose

homeostasis (Figure 3F, 4H), suggesting that GIP receptors remain responsive in the obese state despite high circulating plasma GIP levels.

Early work showed that administration of exogenous GIP failed to stimulate insulin secretion in patients with T2D (71). This finding prompted the speculation that β-cell GIP receptors are desensitized or down-regulated in T2D due to high circulating levels of GIP (reviewed in (12, 70). However, Stensen et al. (21) recently showed that treatment of diabetic individuals with a selective GIP receptor antagonist lowered plasma insulin levels after a mixed meal, indicating that endogenous GIP retains considerable insulinotropic activity in T2D. In agreement with this finding, we demonstrated that chronic DCZ treatment of obese K-GsD mice with impaired glucose homeostasis resulted in increases in both plasma GIP and insulin levels (Figure 4E, F). These hormonal changes were accompanied by a marked improvement in glucose tolerance, strongly suggesting that GIP receptor-mediated insulin release is not subject to desensitization under these diabetogenic conditions and that chronic activation of K-cell G_s signaling may prove useful to restore euglycemia in T2D.

We also investigated whether chronic activation of K-cell G_s signaling might improve glucose homeostasis in a mouse model of T2D (STZ-induced reduction in β-cell mass). Strikingly, while STZ+DCZ-treated control mice developed severe hyperglycemia, this response was greatly reduced in STZ+DCZ-treated K-GsD mice (Figure 5E). STZ+DCZ-treated K-GsD mice showed significantly elevated plasma GIP and insulin levels, as compared to STZ+DCZ treated control mice (Figure 5F, G). These data suggest that the beneficial metabolic effects observed after chronic activation of K-cell G_s signaling in this mouse model of diabetes are mediated by GIP-dependent stimulation of insulin secretion.

Many studies have shown that a fat-rich meal strongly stimulates the secretion of GIP from K-cells (reviewed in (6, 52, 65)). In agreement with this finding, we showed that oral administration of olive oil resulted in increased plasma GIP levels in control mice (Figure 7H). Interestingly, this response was greatly attenuated in K-Gs-KO mice (Figure 7H), suggesting that long-chain fatty acids or monoacylglycerols released by the enzymatic breakdown of the triglycerides contained in olive oil primarily act by stimulating K-cell G_s signaling to exert their stimulatory effect on GIP release. K-cells express GPCRs for several long-chain fatty acids and monoacylglycerols, including FFAR1 (GPR40), FFAR4 (GR120), and GPR119 (65). Whereas the activation of FFAR1 and FFAR4 by long-chain fatty acids preferentially leads to the stimulation of G proteins of the G_q family, the binding of monoacylglycerols to GPR119 triggers the activation of G_s (65, 72). Taken together, these data suggest that the ingestion of a fat-rich meal triggers GIP release primarily by promoting K-cell G_s signaling, probably involving the activation of GPR119. In future studies, we are planning to further test this hypothesis by generating and analyzing K-cell-specific *Gpr119* knockout mice.

In agreement with the phenotypes displayed by the K-GsD mice, mice selectively lacking $G\alpha_s$ in K-cells (K-Gs-KO mice) showed significant reductions in plasma GIP levels, consistent with the important role of G_s in regulating K-cell function. Refeeding studies showed that control mice displayed markedly elevated plasma GIP levels at the end of the 2-hour refeeding period, whereas plasma GIP levels remained unchanged in K-Gs-KO mice under these experimental conditions (Figure 6N). In agreement with this observation, the refeeding-induced hyperglycemia was significantly elevated in K-Gs-KO mice, as compared with their control littermates (Figure 6L). This observation clearly indicates that K-cell G_s signaling plays a physiological role in suppressing meal-induced blood glucose excursions. However, K-Gs-KO mice did not show

significant changes in body weight, food intake, glucose tolerance, and insulin sensitivity, suggesting that a reduction of plasma GIP levels by about 50% does not affect other metabolic parameters, at least not in mice.

As mentioned in the previous paragraph, K-Gs-KO mice showed residual GIP production. It is well documented that GIP release is triggered not only by receptor-mediated activation of G_s signaling in K-cells, but also by activation of receptors linked to G proteins of the G_q family, including FFAR1 (Supplemental Figure 7) (reviewed in (6)). Moreover, many nutrients including glucose, peptides, and amino acids promote GIP secretion via G protein-independent mechanisms (6), explaining why GIP release still occurs in K-Gs-KO mice. The observation that reduced GIP secretion did not affect glucose tolerance in lean female and obese male K-Gs-KO mice is most likely due to the ability of GLP1 and/or other signaling molecules to compensate for the reduction in plasma GIP levels caused by the lack of K-cell G_s signaling.

While most studies described in this manuscript were carried out with male mice, several key experiments were repeated with female mice. These studies showed that DCZ-treated K-GsD mice and K-Gs-KO mice showed similar metabolic changes as their male counterparts (Supplemental Figure 2A-D, 6A-D).

Interestingly, the analysis of published scRNAseq data showed that both mouse and human K-cells express many GPCRs that preferentially couple to G_s. Mouse K-cells express particularly high levels of *Gpr119* which codes for a G_s-coupled receptor that is activated predominantly by breakdown products of triglycerides (Supplemental Figure 8). In the present study, we demonstrated that olive oil-induced GIP release was greatly reduced in K-Gs-KO mice (Figure 7H). A similar phenotype was observed when olive oil was given to *Gpr119* knockout mice (73).

Taken together, these findings suggest that triglyceride-induced GIP release is primarily mediated by activation of K-cell Gpr119, at least in the mouse.

We also identified five G_s-coupled receptors that are expressed in both mouse and human K-cells (Supplemental Figure 8). The G_s-coupled receptors expressed by human K-cells, including the G protein-coupled bile acid receptor 1 (*GPBAR1*) which was expressed at particularly high levels, could emerge as useful targets for developing drugs aimed at enhancing endogenous GIP release for therapeutic purposes.

Of note, both mouse and human K-cells also expressed G_s-coupled GIP receptors (Supplemental Figure 8). In the present study, we demonstrated that stimulation of G_s signalling in K-cells results in a pronounced increase in GIP release. GIP secreted from K-cells is predicted to activate K-cell GIP receptors, leading to a further enhancement of GIP release in a positive feedback loop.

In conclusion, metabolic studies with K-GsD- and K-Gs-KO mice have led to several important findings regarding the mechanisms of GIP release and the metabolic benefits of stimulating endogenous GIP release. Clearly, these data provide a rational basis for the development of drugs that can promote K-cell G_s signaling for the therapy of T2D and related metabolic disorders.

Methods

Sex as a biological variable.

Our study examined male and female mice, and similar findings were obtained for both sexes.

Mouse maintenance.

Mice were group-housed at 23ºC and fed *ad libitum* on a 12-hour light/12-hour dark cycle. Most studies were carried out with mice consuming regular chow diet (7022 NIH-07, 15% kcal fat, energy density 3.1 kcal/g, Envigo Inc.). A subgroup of mice was maintained on a high-fat diet (HFD; F3282, 60% kcal fat, energy density 5.5 kcal/g, Bioserv) after reaching 8 weeks of age. Metabolic studies were performed with mice that were at least 8 weeks old.

Generation of K-cell-specific Gs DREADD (GsD) and Gα_s knockout mice.

To generate K-cell specific GsD mice, homozygous *ROSA26-LSL-Gs-DREADD-CRE-luc* (short name: LSL-GsD) mice (32) were crossed with *Gip-Cre* mice that express Cre recombinase under the transcriptional control of the *Gip* promotor (33). *Cre*-positive hemizygous LSL-GsD mice (K-GsD mice) are predicted to express the GsD designer receptor selectively in K-cells. LSL-GsD mice lacking the *Cre* transgene served as control littermates.

To inactivate *Gnas* (encoded protein: Gα_s) selectively in K-cells, we crossed floxed *Gnas* mice (*Gnas*$^{flox/flox}$ mice) (50) with *Gip-Cre* mice (33). The resulting *Cre*-positive *Gnas*$^{flox/+}$ mice were then backcrossed to *Gnas*$^{flox/flox}$ mice. *Cre*-positive *Gnas*$^{flox/flox}$ mice (K-Gs-KO mice) are predicted to harbor an inactive version of *Gnas* selectively in K-cells. *Gnas*$^{flox/flox}$ mice that did not carry the *Cre* transgene were used as control littermates. Mouse tail DNA was used for PCR

genotyping of *Gip-Cre*, *Gnas*$^{flox/flox}$, and LSL-GsD mice. PCR reactions were carried out using standard procedures. Primer sequences are given in Supplemental Table 1.

All mice used for these matings had been backcrossed for at least 7 times onto a C57BL/6 background.

All other experimental procedures are desribed in Supplemental Data (Supplemental Methods).

Statistics

Data are expressed as means ± SEM for the indicated number of observations. Data were assessed for statistical significance by 2-way-ANOVA, followed by the indicated post-hoc tests, or by using a two-tailed unpaired Student's t-test, as appropriate. A P value of <0.05 was considered statistically significant. The specific statistical tests that were used are indicated in the figure legends.

Study approval

All animal experiments were conducted according to the US National Institutes of Health Guidelines for Animal Research and were approved by the NIDDK Institutional Animal Care and Use Committee.

Data availability

All data are available in the main text or the supplemental materials. Values for all data points in graphs are reported in the Supporting Data Values file.

Author contributions

ABO and JW conceived and designed the study. ABO performed most of the experiments, with help from LL, YC, HL, NG, OG, and JL. FR, FG, MC, LW, and JC provided mouse models or reagents and helpful advice throughout this study. ABO wrote the first draft of the manuscript. ABO and JW jointly finalized the manuscript.

Acknowledgments

This research was funded by the Intramural Research Program of the National Institute of Diabetes and Digestive and Kidney Diseases (AOB, LL, YC, OG, HL, MC, LW, and JW; NIDDK, NIH). Research in the Reimann/Gribble laboratories is funded by Wellcome (220271/Z/20/Z) and the Medical Research Council UK (MRC_MC_UU_12012/3). We thank AstraZeneca for generously providing the monoclonal antibodies against the GIP receptor (GIPg013) and the GLP1 receptor (Glp10017), respectively. Dr. Yoko Hamazaki (Kyoto University, Japan) kindly provided the biotinylated anti-claudin4 antibody needed for the isolation of mouse duodenal K-cells. Dr. Thue Schwartz (University of Copenhagen, Denmark) kindly provided the AM1638 compound. We also thank Tamar Demby (Mouse Metabolism Core, NIDDK) for expert technical assistance and the members of the NIDDK Biostatistics Program, including Dr. Sungyoung Auh, for their help regarding statistics-related questions, respectively.

Address correspondence to:

Dr. Jürgen Wess

Laboratory of Bioorganic Chemistry

Molecular Signaling Section, National Institute of Diabetes and Digestive and Kidney Diseases

Bldg. 8A, Room B1A-05, 8 Center Drive
Bethesda, Maryland 20892, USA
Email: jurgenw@niddk.nih.gov

References

1. Alsalim W, Lindgren O, and Ahrén B. Glucose-dependent insulinotropic polypeptide and glucagon-like peptide-1 secretion in humans: Characteristics and regulation. *J Diabet Invest.* 2023;14(3):354-61.
2. Gribble FM, and Reimann F. Function and mechanisms of enteroendocrine cells and gut hormones in metabolism. *Nat Rev Endocrinol.* 2019;15(4):226-37.
3. Holst JJ. The incretin system in healthy humans: The role of GIP and GLP-1. *Metabolism: Clin Experim.* 2019;96:46-55.
4. Drucker DJ, and Holst JJ. The expanding incretin universe: from basic biology to clinical translation. *Diabetologia.* 2023;66(10):1765-79.
5. Samms RJ, Sloop KW, Gribble FM, Reimann F, and Adriaenssens AE. GIPR Function in the central nervous system: implications and novel perspectives for GIP-based therapies in treating metabolic disorders. *Diabetes.* 2021;70(9):1938-44.
6. Guccio N, Gribble FM, and Reimann F. Glucose-Dependent Insulinotropic Polypeptide-A Postprandial Hormone with Unharnessed Metabolic Potential. *Ann Rev Nutr.* 2022;42:21-44.
7. Alexander SPH, Christopoulos A, Davenport AP, Kelly E, Mathie AA, Peters JA, et al. The Concise Guide to PHARMACOLOGY 2023/24: G protein-coupled receptors. *Br J Pharmacol.* 2023;180 Suppl 2:S23-s144.
8. Holst JJ, Gasbjerg LS, and Rosenkilde MM. The role of incretins on insulin function and glucose homeostasis. *Endocrinology.* 2021;162(7).
9. Drucker DJ. GLP-1 physiology informs the pharmacotherapy of obesity. *Mol Metab.* 2022;57:101351.
10. Drucker DJ. Mechanisms of action and therapeutic application of glucagon-like peptide-1. *Cell Metab.* 2018;27(4):740-56.
11. Knop FK, Aaboe K, Vilsboll T, Volund A, Holst JJ, Krarup T, et al. Impaired incretin effect and fasting hyperglucagonaemia characterizing type 2 diabetic subjects are early signs of dysmetabolism in obesity. *Diabetes Obes Metab.* 2012;14(6):500-10.
12. Finan B, Müller TD, Clemmensen C, Perez-Tilve D, DiMarchi RD, and Tschöp MH. Reappraisal of GIP pharmacology for metabolic diseases. *Trends Mol Med.* 2016;22(5):359-76.

13. Campbell JE. Targeting the GIPR for obesity: To agonize or antagonize? Potential mechanisms. *Mol Metab.* 2021;46:101139.
14. Miyawaki K, Yamada Y, Ban N, Ihara Y, Tsukiyama K, Zhou H, et al. Inhibition of gastric inhibitory polypeptide signaling prevents obesity. *Natu Med.* 2002;8(7):738-42.
15. Nasteska D, Harada N, Suzuki K, Yamane S, Hamasaki A, Joo E, et al. Chronic reduction of GIP secretion alleviates obesity and insulin resistance under high-fat diet conditions. *Diabetes.* 2014;63(7):2332-43.
16. Turcot V, Lu Y, Highland HM, Schurmann C, Justice AE, Fine RS, et al. Protein-altering variants associated with body mass index implicate pathways that control energy intake and expenditure in obesity. *Nat Genet.* 2018;50(1):26-41.
17. Gaffey RH, Takyi AK, and Shukla A. Investigational and emerging gastric inhibitory polypeptide (GIP) receptor-based therapies for the treatment of obesity. *Expert Opin Investig Drugs.* 2024;33(8):757-73.
18. Frías JP, Davies MJ, Rosenstock J, Pérez Manghi FC, Fernández Landó L, Bergman BK, et al. Tirzepatide versus semaglutide once weekly in patients with type 2 diabetes. *New Engl J Med.* 2021;385(6):503-15.
19. Heise T, Mari A, DeVries JH, Urva S, Li J, Pratt EJ, et al. Effects of subcutaneous tirzepatide versus placebo or semaglutide on pancreatic islet function and insulin sensitivity in adults with type 2 diabetes: a multicentre, randomised, double-blind, parallel-arm, phase 1 clinical trial. *Lancet Diabetes Endocrinol.* 2022;10(6):418-29.
20. Højberg PV, Vilsbøll T, Rabøl R, Knop FK, Bache M, Krarup T, et al. Four weeks of near-normalisation of blood glucose improves the insulin response to glucagon-like peptide-1 and glucose-dependent insulinotropic polypeptide in patients with type 2 diabetes. *Diabetologia.* 2009;52(2):199-207.
21. Stensen S, Gasbjerg LS, Krogh LL, Skov-Jeppesen K, Sparre-Ulrich AH, Jensen MH, et al. Effects of endogenous GIP in patients with type 2 diabetes. *Eur J Endocrinol.* 2021;185(1):33-45.
22. Reimann F, Tolhurst G, and Gribble FM. G-protein-coupled receptors in intestinal chemosensation. *Cell Metab.* 2012;15(4):421-31.
23. Regard JB, Sato IT, and Coughlin SR. Anatomical profiling of G protein-coupled receptor expression. *Cell.* 2008;135(3):561-71.

24. Armbruster BN, Li X, Pausch MH, Herlitze S, and Roth BL. Evolving the lock to fit the key to create a family of G protein-coupled receptors potently activated by an inert ligand. *Proc Natl Acad Sci U S A.* 2007;104(12):5163-8.
25. Guettier JM, Gautam D, Scarselli M, Ruiz de Azua I, Li JH, Rosemond E, et al. A chemical-genetic approach to study G protein regulation of beta cell function in vivo. *Proc Natl Acad Sci U S A.* 2009;106(45):19197-202.
26. Urban DJ, and Roth BL. DREADDs (designer receptors exclusively activated by designer drugs): chemogenetic tools with therapeutic utility. *Annu Rev Pharmacol Toxicol.* 2015;55:399-417.
27. Kang HJ, Minamimoto T, Wess J, and Roth BL. Chemogenetics for cell-type-specific modulation of signalling and neuronal activity. *Nat Rev Meth Primers.* 2023;3(1).
28. Inoue A, Raimondi F, Kadji FMN, Singh G, Kishi T, Uwamizu A, et al. Illuminating G-Protein-Coupling Selectivity of GPCRs. *Cell.* 2019;177(7):1933-47.e25.
29. Wang L, Zhu L, Meister J, Bone DBJ, Pydi SP, Rossi M, et al. Use of DREADD technology to identify novel targets for antidiabetic drugs. *Annu Rev Pharmacol Toxicol.* 2021;61:421-40.
30. Nagai Y, Miyakawa N, Takuwa H, Hori Y, Oyama K, Ji B, et al. Deschloroclozapine, a potent and selective chemogenetic actuator enables rapid neuronal and behavioral modulations in mice and monkeys. *Nat Neurosci.* 2020;23(9):1157-67.
31. Shimizu M, Yoshimura M, Baba K, Ikeda N, Nonaka Y, Maruyama T, et al. Deschloroclozapine exhibits an exquisite agonistic effect at lower concentration compared to clozapine-N-oxide in hM3Dq expressing chemogenetically modified rats. *Front Neurosci.* 2023;17:1301515..
32. Akhmedov D, Mendoza-Rodriguez MG, Rajendran K, Rossi M, Wess J, and Berdeaux R. Gs-DREADD knock-in mice for tissue-specific, temporal stimulation of cyclic AMP Signaling. *Mol Cell Biol.* 2017;37(9).
33. Svendsen B, Pais R, Engelstoft MS, Milev NB, Richards P, Christiansen CB, et al. GLP1- and GIP-producing cells rarely overlap and differ by bombesin receptor-2 expression and responsiveness. *J Endo.* 2016;228(1):39-48.

34. Nagai Y, Miyakawa N, Takuwa H, Hori Y, Oyama K, Ji B, et al. Deschloroclozapine, a potent and selective chemogenetic actuator enables rapid neuronal and behavioral modulations in mice and monkeys. *Nat Neurosci.* 2020; 23(9):1157-1167.
35. Asmar M, and Holst JJ. Glucagon-like peptide 1 and glucose-dependent insulinotropic polypeptide: new advances. *Curr Opin Endocrinol Diabetes Obes.* 2010;17(1):57-62.
36. Khan R, Tomas A, and Rutter GA. Effects on pancreatic beta and other islet cells of the glucose-dependent insulinotropic polypeptide. *Peptides.* 2020;125:170201.
37. Smits MM, Galsgaard KD, Jepsen SL, Albrechtsen NW, Hartmann B, and Holst JJ. In vivo inhibition of dipeptidyl peptidase 4 allows measurement of GLP-1 secretion in mice. *Diabetes.* 2024; 73(5):671-681.
38. Svendsen B, Capozzi ME, Nui J, Hannou SA, Finan B, Naylor J, et al. Pharmacological antagonism of the incretin system protects against diet-induced obesity. *Mol Metab.* 2020;32:44-55.
39. Ravn P, Madhurantakam C, Kunze S, Matthews E, Priest C, O'Brien S, et al. Structural and pharmacological characterization of novel potent and selective monoclonal antibody antagonists of glucose-dependent insulinotropic polypeptide receptor. *J Biol Chem.* 2013;288(27):19760-72.
40. Fukuda M. The role of GIP Receptor in the CNS for the pathogenesis of obesity. *Diabetes.* 2021;70(9):1929-37.
41. Jain S, Ruiz de Azua I, Lu H, White MF, Guettier JM, and Wess J. Chronic activation of a designer G(q)-coupled receptor improves beta cell function. *J Clin Invest.* 2013;123(4):1750-62.
42. Maida A, Hansotia T, Longuet C, Seino Y, and Drucker DJ. Differential importance of glucose-dependent insulinotropic polypeptide vs glucagon-like peptide 1 receptor signaling for beta cell survival in mice. *Gastroenterology.* 2009;137(6):2146-57.
43. Butler AE, Janson J, Bonner-Weir S, Ritzel R, Rizza RA, and Butler PC. Beta-cell deficit and increased beta-cell apoptosis in humans with type 2 diabetes. *Diabetes.* 2003;52(1):102-10.
44. Hrovatin K, Bastidas-Ponce A, Bakhti M, Zappia L, Büttner M, Salinno C, et al. Delineating mouse β-cell identity during lifetime and in diabetes with a single cell atlas. *Nat Metab.* 2023;5(9):1615-37.

45. Campbell JE, Ussher JR, Mulvihill EE, Kolic J, Baggio LL, Cao X, et al. TCF1 links GIPR signaling to the control of beta cell function and survival. *Nat Med.* 2016;22(1):84-90.
46. Villhauer EB, Brinkman JA, Naderi GB, Burkey BF, Dunning BE, Prasad K, et al. 1-[[(3-hydroxy-1-adamantyl)amino]acetyl]-2-cyano-(S)-pyrrolidine: a potent, selective, and orally bioavailable dipeptidyl peptidase IV inhibitor with antihyperglycemic properties. *Journal Med Chem.* 2003;46(13):2774-89.
47. Hinke SA, Gelling RW, Pederson RA, Manhart S, Nian C, Demuth HU, et al. Dipeptidyl peptidase IV-resistant [D-Ala(2)]glucose-dependent insulinotropic polypeptide (GIP) improves glucose tolerance in normal and obese diabetic rats. *Diabetes.* 2002;51(3):652-61.
48. Sarnobat D, Moffett RC, Gault VA, Tanday N, Reimann F, Gribble FM, et al. Effects of long-acting GIP, xenin and oxyntomodulin peptide analogues on alpha-cell transdifferentiation in insulin-deficient diabetic Glu(CreERT2);ROSA26-eYFP mice. *Peptides.* 2020;125:170205.
49. Kerr BD, Flatt AJ, Flatt PR, and Gault VA. Characterization and biological actions of N-terminal truncated forms of glucose-dependent insulinotropic polypeptide. *Biochem Biophys Res Commun.* 2011;404(3):870-6.
50. Chen M, Gavrilova O, Zhao WQ, Nguyen A, Lorenzo J, Shen L, et al. Increased glucose tolerance and reduced adiposity in the absence of fasting hypoglycemia in mice with liver-specific Gs alpha deficiency. *J Clin Invest.* 2005;115(11):3217-27.
51. Nagatake T, Fujita H, Minato N, and Hamazaki Y. Enteroendocrine cells are specifically marked by cell surface expression of claudin-4 in mouse small intestine. *PLoS One.* 2014;9(6):e90638.
52. Marks V. The early history of GIP 1969-2000: From enterogastrone to major metabolic hormone. *Peptides.* 2020;125:170276.
53. Lewis JE, Nuzzaci D, James-Okoro PP, Montaner M, O'Flaherty E, Darwish T, et al. Stimulating intestinal GIP release reduces food intake and body weight in mice. *Mol Metab.* 2024;84:101945.

54. Hauge M, Vestmar MA, Husted AS, Ekberg JP, Wright MJ, Di Salvo J, et al. GPR40 (FFAR1) - Combined Gs and Gq signaling in vitro is associated with robust incretin secretagogue action ex vivo and in vivo. *Mol Metab.* 2015;4(1):3-14.
55. Luo J, Swaminath G, Brown SP, Zhang J, Guo Q, Chen M, et al. A potent class of GPR40 full agonists engages the enteroinsular axis to promote glucose control in rodents. *PLoS One.* 2012;7(10):e46300.
56. Hayashi M, Kaye JA, Douglas ER, Joshi NR, Gribble FM, Reimann F, et al. Enteroendocrine cell lineages that differentially control feeding and gut motility. *Elife.* 2023;12.
57. Beumer J, Puschhof J, Bauzá-Martinez J, Martínez-Silgado A, Elmentaite R, James KR, et al. High-resolution mRNA and secretome atlas of human enteroendocrine cells. *Cell.* 2020;182(4):1062-4.
58. Jacob S, and Varughese GI. Tirzepatide, the newest medication for type 2 diabetes: a review of the literature and implications for clinical practice. *Ann Pharmacother.* 2024:10600280231224039.
59. Nauck MA, and D'Alessio DA. Tirzepatide, a dual GIP/GLP-1 receptor co-agonist for the treatment of type 2 diabetes with unmatched effectiveness regrading glycaemic control and body weight reduction. *Cardiovasc Diabetol.* 2022;21(1):169.
60. Jastreboff AM, Aronne LJ, Ahmad NN, Wharton S, Connery L, Alves B, et al. Tirzepatide once weekly for the treatment of obesity. *New Engl J Med.* 2022;387(3):205-16.
61. Campbell JE, Müller TD, Finan B, DiMarchi RD, Tschöp MH, and D'Alessio DA. GIPR/GLP-1R dual agonist therapies for diabetes and weight loss-chemistry, physiology, and clinical applications. *Cell Metab.* 2023;35(9):1519-29.
62. Bailey CJ, Flatt PR, and Conlon JM. Recent advances in peptide-based therapies for obesity and type 2 diabetes. *Peptides.* 2024;173:171149.
63. Nauck MA, and Müller TD. Incretin hormones and type 2 diabetes. *Diabetologia.* 2023;66(10):1780-95.
64. El K, Douros JD, Willard FS, Novikoff A, Sargsyan A, Perez-Tilve D, et al. The incretin co-agonist tirzepatide requires GIPR for hormone secretion from human islets. *Nat Metab.* 2023;5(6):945-54.

65. Santos Hernandez M, Reimann F, and Gribble FM. Cellular mechanisms of incretin hormone secretion. *J Mol Endo.* 2024; 72(4):e230112.
66. Sriram K, and Insel PA. G Protein-Coupled Receptors as Targets for Approved Drugs: How Many Targets and How Many Drugs? *Mol Pharmacol.* 2018;93(4):251-8.
67. Miedzybrodzka EL, Foreman RE, Lu VB, George AL, Smith CA, Larraufie P, et al. Stimulation of motilin secretion by bile, free fatty acids, and acidification in human duodenal organoids. *Mol Metab.* 2021;54:101356.
68. Calanna S, Christensen M, Holst JJ, Laferrère B, Gluud LL, Vilsbøll T, et al. Secretion of glucose-dependent insulinotropic polypeptide in patients with type 2 diabetes: systematic review and meta-analysis of clinical studies. *Diabet Care.* 2013;36(10):3346-52.
69. Salera M, Giacomoni P, Pironi L, Cornia G, Capelli M, Marini A, et al. Gastric inhibitory polypeptide release after oral glucose: relationship to glucose intolerance, diabetes mellitus, and obesity. *J Clin Endo Metab.* 1982;55(2):329-36.
70. Holst JJ, Albrechtsen NJW, Rosenkilde MM, and Deacon CF. Physiology of the incretin hormones, GIP and GLP-1-regulation of release and posttranslational modifications. *Compr Physiol.* 2019;9(4):1339-81.
71. Nauck MA, Heimesaat MM, Orskov C, Holst JJ, Ebert R, and Creutzfeldt W. Preserved incretin activity of glucagon-like peptide 1 [7-36 amide] but not of synthetic human gastric inhibitory polypeptide in patients with type-2 diabetes mellitus. *J Clin Invest.* 1993;91(1):301-7.
72. Oteng AB, and Liu L. GPCR-mediated effects of fatty acids and bile acids on glucose homeostasis. *Front Endocrinol (Lausanne).* 2023;14:1206063.
73. Ekberg JH, Hauge M, Kristensen LV, Madsen AN, Engelstoft MS, Husted AS, et al. GPR119, a major enteroendocrine sensor of dietary triglyceride metabolites coacting in synergy with FFA1 (GPR40). *Endocrinology.* 2016;157(12):4561-9.

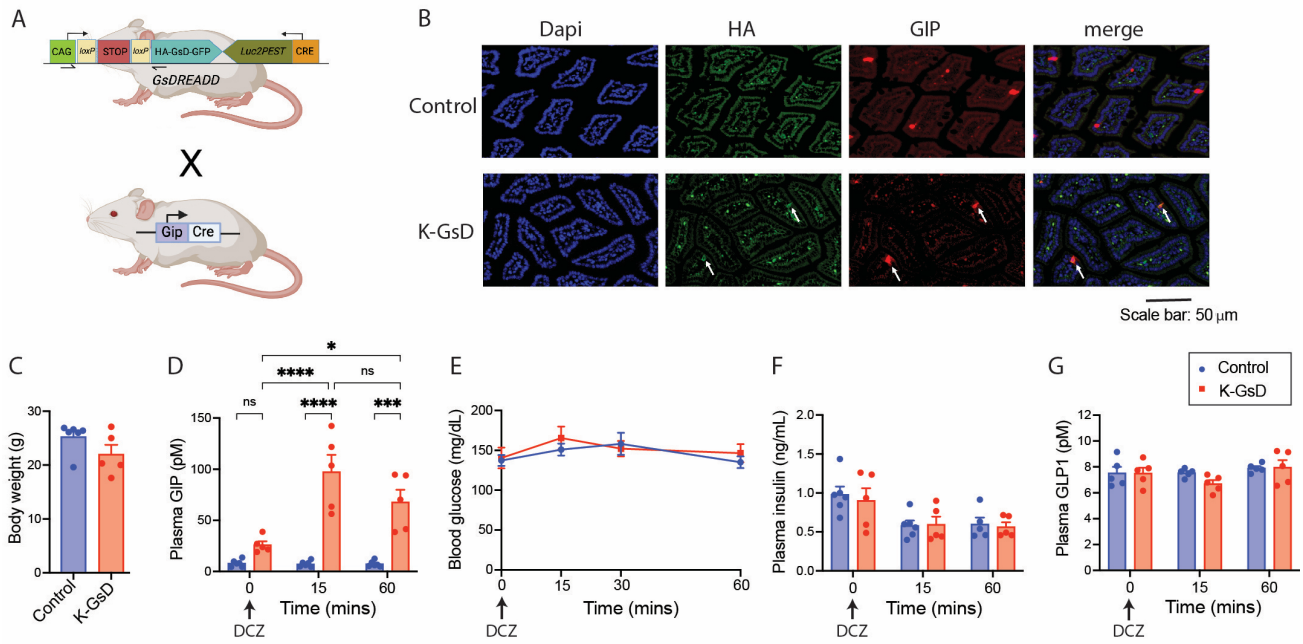

Figure 1. Selective activation of the GsD designer receptor in K-cells stimulates GIP secretion in vivo. (A) Scheme depicting the generation of mice selectively expressing the GsD DREADD in K-cells. **(B)** Representative immunohistochemical images showing co-localization of GIP and GsD (detected with an anti-HA antibody directed against the HA tag fused to the N-terminus of GsD) in the duodenal epithelium of K-GsD mice but not control littermates. White arrows point at individual K-cells expressing GsD. Note that the anti-HA antibody caused marked non-specific staining (staining seen in both control and K-GsD mice). **(C)** Body weight of 8-week-old K-GsD mice and control littermates consuming regular chow. (**D-G**) Treatment of K-GsD mice and control littermates with a single oral dose of DCZ (10 µg/kg). Changes in plasma GIP (**D**), blood glucose (**E**), plasma insulin (**F**), and plasma GLP1 (**G**) levels were monitored at the indicated time points. All experiments were performed with male mice after a 6-hour fast. Data are given as means ± SEM (n = 5 or 6 mice/group). *P<0.05, ***P<0.001, ****P<0.0001; 2-way ANOVA followed by Tukey post-hoc analysis. ns, no statistically significant difference.

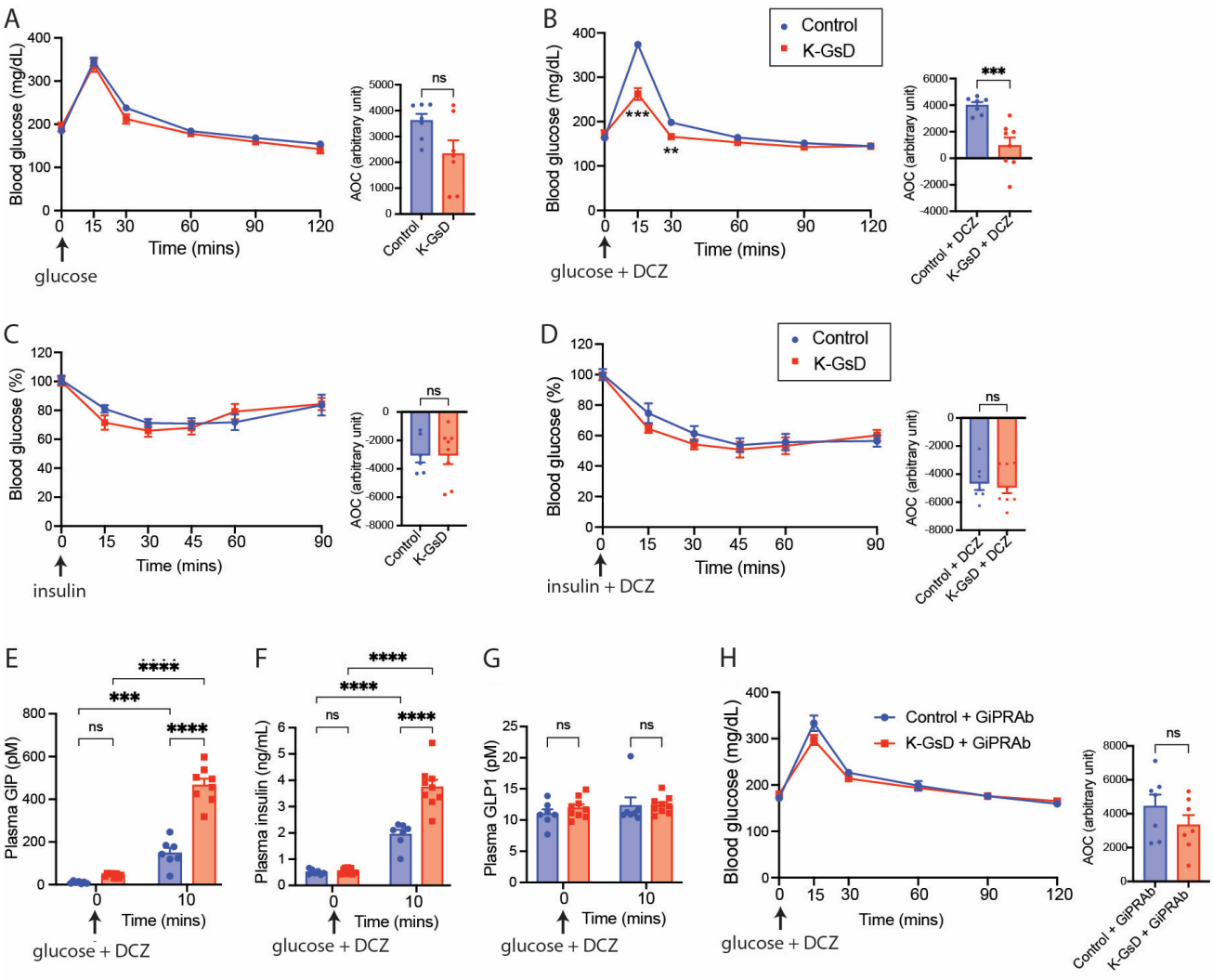

Figure 2. Stimulation of K-cell G_s signaling results in improved glucose tolerance in lean K-GsD mice. (A, B) Oral glucose tolerance tests (OGTT). In (**A**), K-GsD mice and control littermates received glucose only (2 g/kg). In (**B**), both groups of mice were treated with glucose plus oral DCZ (10 µg/kg). **(C, D)** Insulin tolerance tests (ITT)**.** In (**C**), K-GsD and control mice received insulin only **(**0.75 U/kg, i.p.). In (**D**), both groups of mice received i.p. insulin plus DCZ (10 µg/kg). AOC values are given as quantitative measures of the experimental data shown in panels (**A-D**). **(E-G)** Co-treatment of K-GsD and control mice with oral glucose plus DCZ (10 µg/kg). Plasma GIP (**E**), plasma insulin (**F**), and plasma GLP1 (**G**) levels were measured at the indicated time points. **(H)** OGTT after oral co-administration of glucose and DCZ 48 hours after treatment with a GIP receptor antibody (GIPRAb). All experiments were carried out with male mice after a 6-hour fast (the fasting period was only 4 hours for ITT studies). Data are given as means ± SEM (n = 7 or 8 mice/group). *P<0.05, **P<0.01, ***P<0.001, ****P<0.0001; 2-way ANOVA followed by Tukey post-hoc analysis (**E-G**) or Student's t-test (**A-D, H**). ns, no statistically significant difference; AOC, area of the curve.

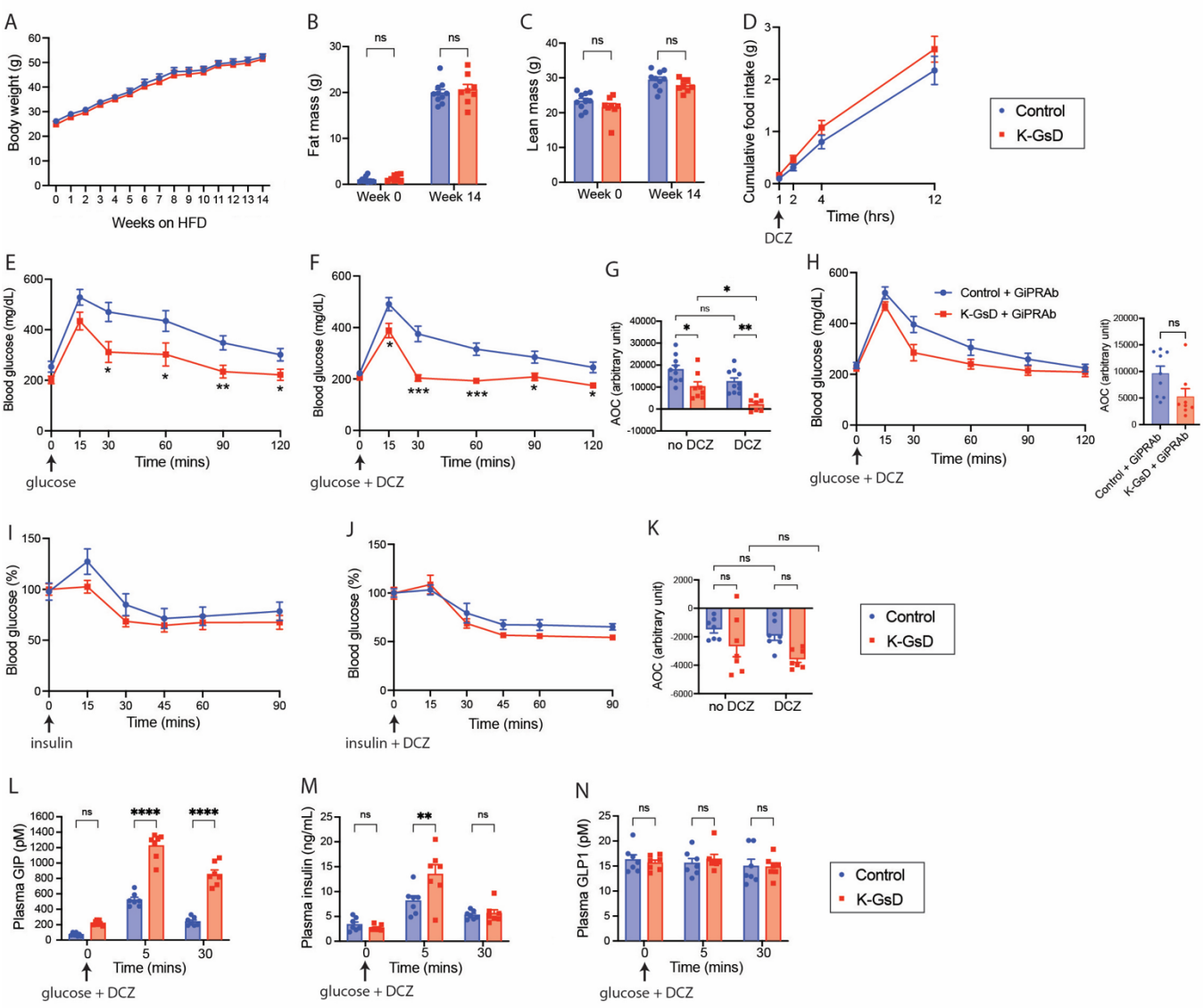

Figure 3. Activation of K-cell G_s signaling greatly improves impaired glucose tolerance in obese K-GsD mice. (A) Body weight gain of 8-week-old K-GsD and control mice consuming a HFD for 14 weeks. **(B, C)** Fat mass (**B**) and lean mass (**C**) before and after HFD feeding. **(D)** Cumulative food intake measured for 12 hours after treatment with an oral bolus of DCZ (10 µg/kg in PBS). **(E-H)** Oral glucose tolerance tests (OGTT). In (**E**), obese K-GsD mice and control littermates received glucose only (1 g/kg). In (**F**), both groups of mice were co-treated with glucose plus DCZ (10 µg/kg). (**G**) AOC values for the data shown in panels (**E**) and (**F**). In (**H**), both groups of mice were co-treated with glucose plus DCZ (10 µg/kg) or saline (control), 48 hours after treatment with a GIP receptor antibody (GIPRAb) or PBS (control). **(I-K)** Insulin tolerance tests (ITT). In (**I**), obese K-GsD and control mice received insulin alone **(**1.5 U/kg,

i.p.). In (**J**), both groups of mice received i.p. insulin plus DCZ (10 μg/kg). **(K**) AOC values for the data shown in panels (**I**) and (**J**). **(L-N)** Co-treatment of obese K-GsD and control mice with oral glucose (1 g/kg) plus DCZ (10 μg/kg). Plasma levels of GIP (**L**), insulin (**M**), and GLP1 (**N**) were measured at the indicated time points. All experiments were performed with obese male mice after a 6-hour fast (the fasting period was only 4 hours for ITT studies). Data are given as means ± SEM (n = 7-10 mice/group). *P<0.05, **P<0.01, ***P<0.001, ****P<0.0001; 2-way ANOVA followed by Tukey post-hoc analysis or Student's t-test (**H**). ns, no statistically significant difference; AOC, area of the curve.

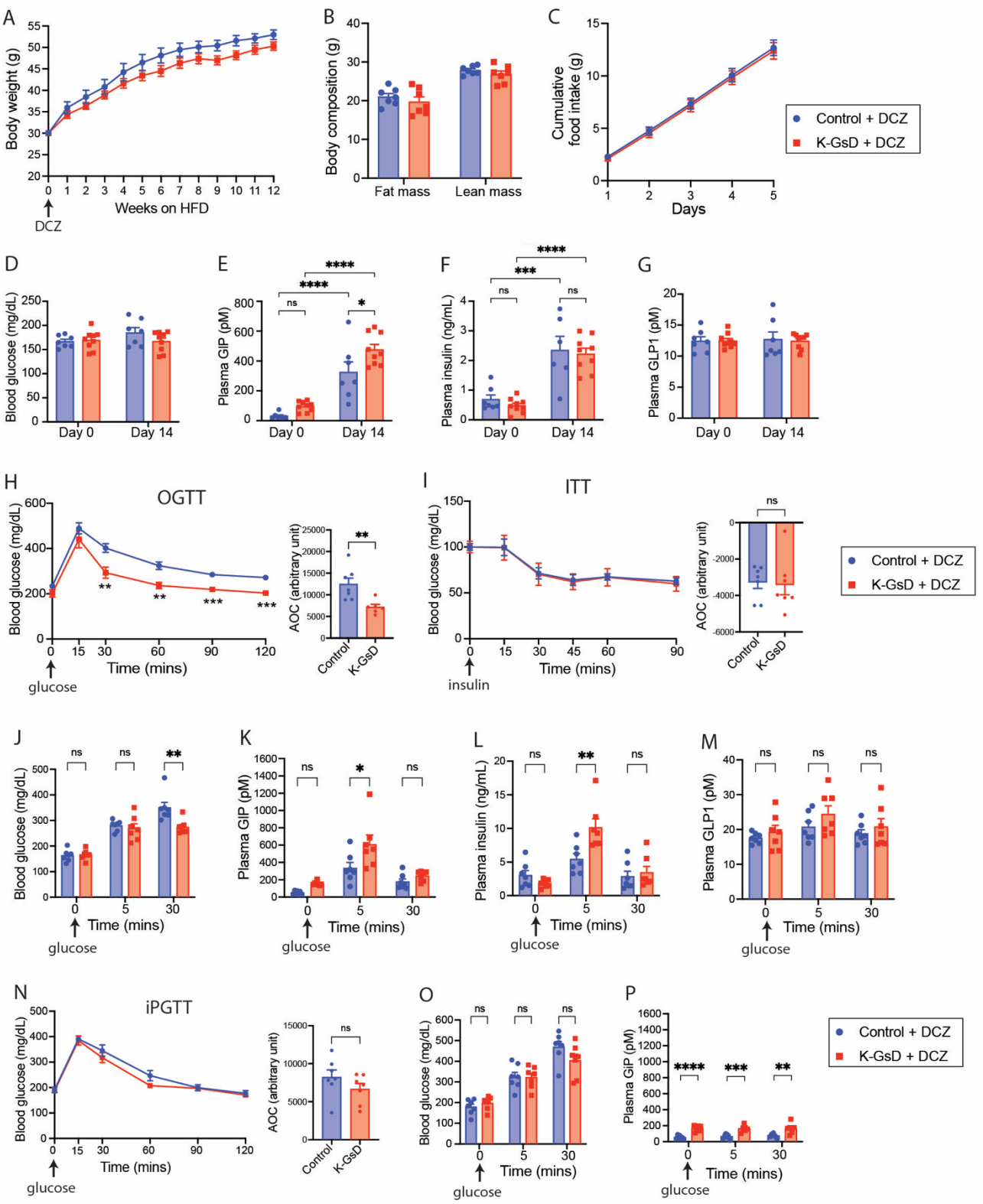

Figure 4. Chronic activation of G_s signaling in K-cells improves glucose tolerance in obese K-GsD mice. (**A**) Body weight gain of 12-week-old K-GsD and control littermates maintained

on HFD and DCZ drinking water for 12 weeks. (**B**) Fat and lean mass after 11 weeks of HFD feeding. (**C**) Cumulative food intake of single-housed mice maintained on the HFD for 11 weeks. (**C**). **(D-H)** Blood glucose (**D**), and plasma levels of GIP (**E**), insulin (**F**), and GLP1 (**G**) in non-fasted mice consuming DCZ drinking water. Measurements were made 14 days after the initiation of HFD feeding. (**H**, **I)** Oral glucose tolerance test (1 g/kg) (**H**) and insulin tolerance test **(**1.5 U/kg, i.p.) (**I**) after 8-9 weeks of HFD feeding carried out with K-GsD and control mice consuming DCZ drinking water. AOC values are shown to the right in each panel. (**J-M)** Blood glucose (**J**), and plasma levels of GIP (**K**), insulin (**L**), and GLP1 (**M**) immediately before (time '0') and after 5 and 30 min of oral administration of glucose (1 g/kg) in mice consuming DCZ drinking water and HFD for 10 weeks. (**N-Q)** I.p. glucose tolerance test (1 g/kg) (**N**), blood glucose levels (**O**), and plasma levels of GIP (**P**) and insulin (**Q**) immediately before (time '0') and after an i.p. glucose bolus (1 g/kg) in mice consuming DCZ drinking water and HFD for 11 weeks. All experiments were performed with male mice after a 6-hour fast (the fasting period was only 4 hours for ITT studies) (**A, B, H-P**). In (**C-G),** mice had free access to food. Data are given as means ± SEM (n = 7-9 mice/group). *P<0.05, **P<0.01, ***P<0.001, ****P<0.0001; 2-way ANOVA followed by Tukey post-hoc analysis (**D-G**, **J-M**, **O-P**) or Student's t-test (**A-C**, **H**, **I**, **N)** *ns, no statistically significant difference; AOC, area of the curve.

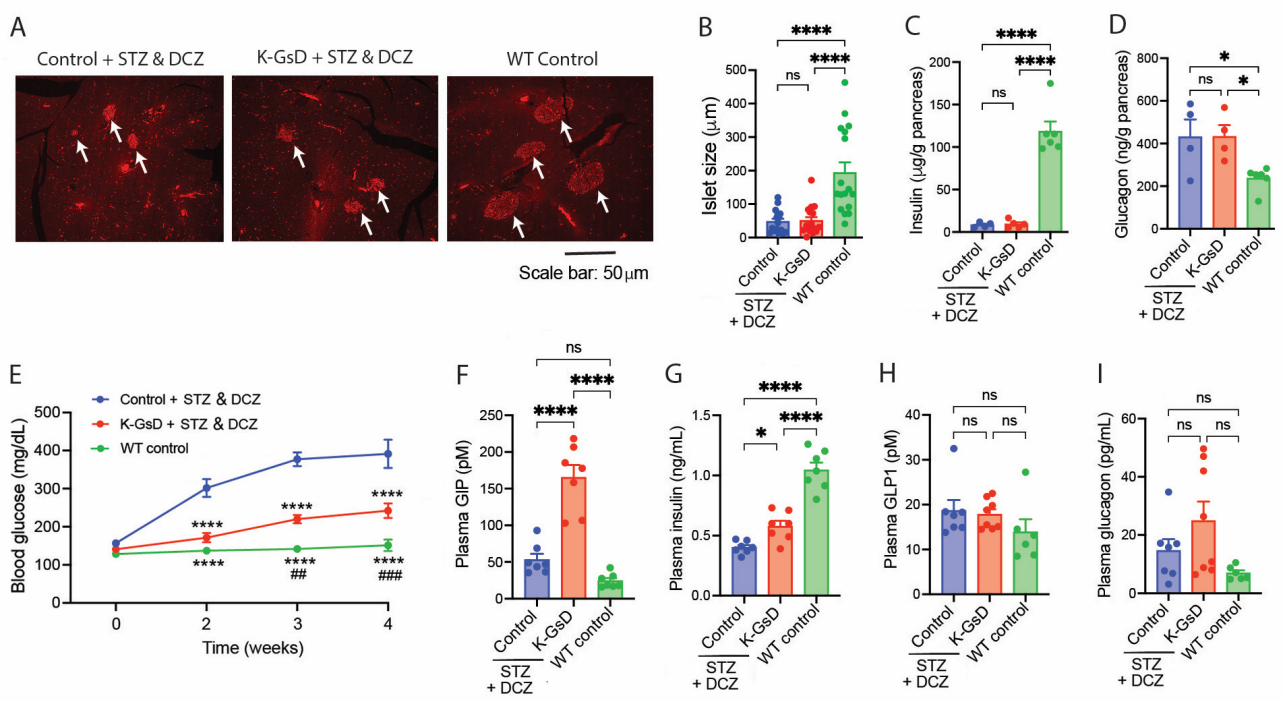

Figure 5. Chronic activation of K-cell G_s signaling greatly reduces STZ-induced hyperglycemia. (**A**) Representative immunofluorescence images showing insulin staining of pancreatic slices from mice of the indicated phenotypes. Healthy, non-STZ-treated WT mice were included for control purposes. (**B**) Quantification of islet size at the end of the treatment period. (**C, D**) Pancreatic content of insulin (**C**) and glucagon (**D**) at the end of the treatment period. (**E**) Suppression of STZ-induced hyperglycemia by cotreatment of K-GsD mice with STZ and DCZ water (10 mg/l). (**F-I**) Plasma levels of GIP (**F**), insulin (**G**), GLP1 (**H**), and glucagon (**I**) at the end of the treatment period. Blood glucose and plasma hormones were measured after a 5-hour fast. In **B**, at least 15 islets from 3 different mice per group were analyzed (n = 4-6 mice/group for **C** and **D**, and 6-8 mice per group for **E-I**, respectively). Data are given as means ± SEM. *P<0.05, **P<0.01, ***P<0.001, ****P<0.0001; 1-way ANOVA (**B-D, F-I**) or 2-way ANOVA **(E)** followed by Tukey post-hoc analysis, respectively. Panel (**E**): ****P<0.0001 relative to control + STZ&DCZ, and $^{\#\#}$P<0.01, $^{\#\#\#}$P<0.001 relative to K-GsD STZ&DCZ, respectively. ns, no statistically significant difference.

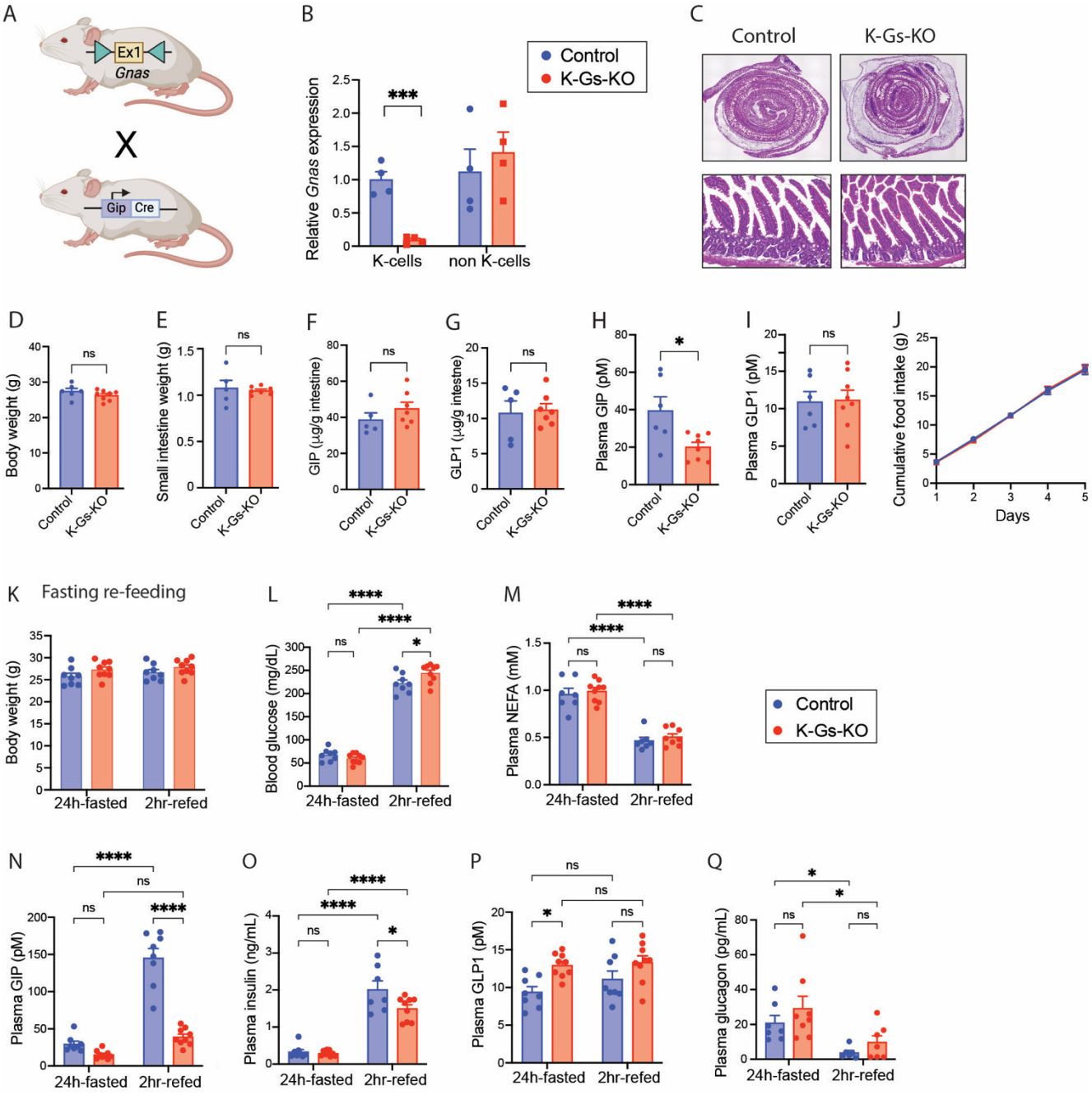

Figure 6. Metabolic studies with K-Gs-KO mice maintained on regular chow. (**A**) Scheme depicting the generation of K-Gs-KO mice that lack Gα_s selectively in enteroendocrine K-cells. (**B**) Transcript levels of *Gnas*, the gene that encodes Gα_s, measured with RNA prepared from duodenal, FACS-sorted K-cells and non-K-cells. (**C**) Representative images of H&E staining experiments showing that the lack of Gα_s in K-cells does not affect the overall morphology of the proximal intestine/duodenum. **(D-G)** K-Gs-KO mice and control littermates show similar

body weight (**D**), whole intestinal weight (**E**), and intestinal content of GIP (**F**) and GLP1 (**G**). (**H, I**) K-Gs-KO mice show reduced plasma GIP levels (**H**), but unchanged plasma GLP1 levels (**I**). (**J**) Food intake measured over 5 days in single-housed mice. **(K-Q)** Metabolic parameters of K-Gs-KO mice and control littermates after refeeding following a 24-hour fast. Body weight (**K**), blood glucose levels (**L**), and plasma levels of NEFAs (**M**), GIP (**N**), insulin (**O**), GLP1 (**P**), and glucagon (**Q**). All experiments were performed with male mice. In (**B-I**), mice were subjected to a 6-hour fast (the fasting period was only 4 hours for ITT studies). Data are given as means ± SEM (n = 7-9 mice/group). *P<0.05, ***P<0.001, ****P<0.0001; 2-way ANOVA followed by Tukey post-hoc analysis (**K-Q**) or Student's t-test (**B, D-J**). ns, no statistically significant difference. NEFA, non-esterified fatty acid.

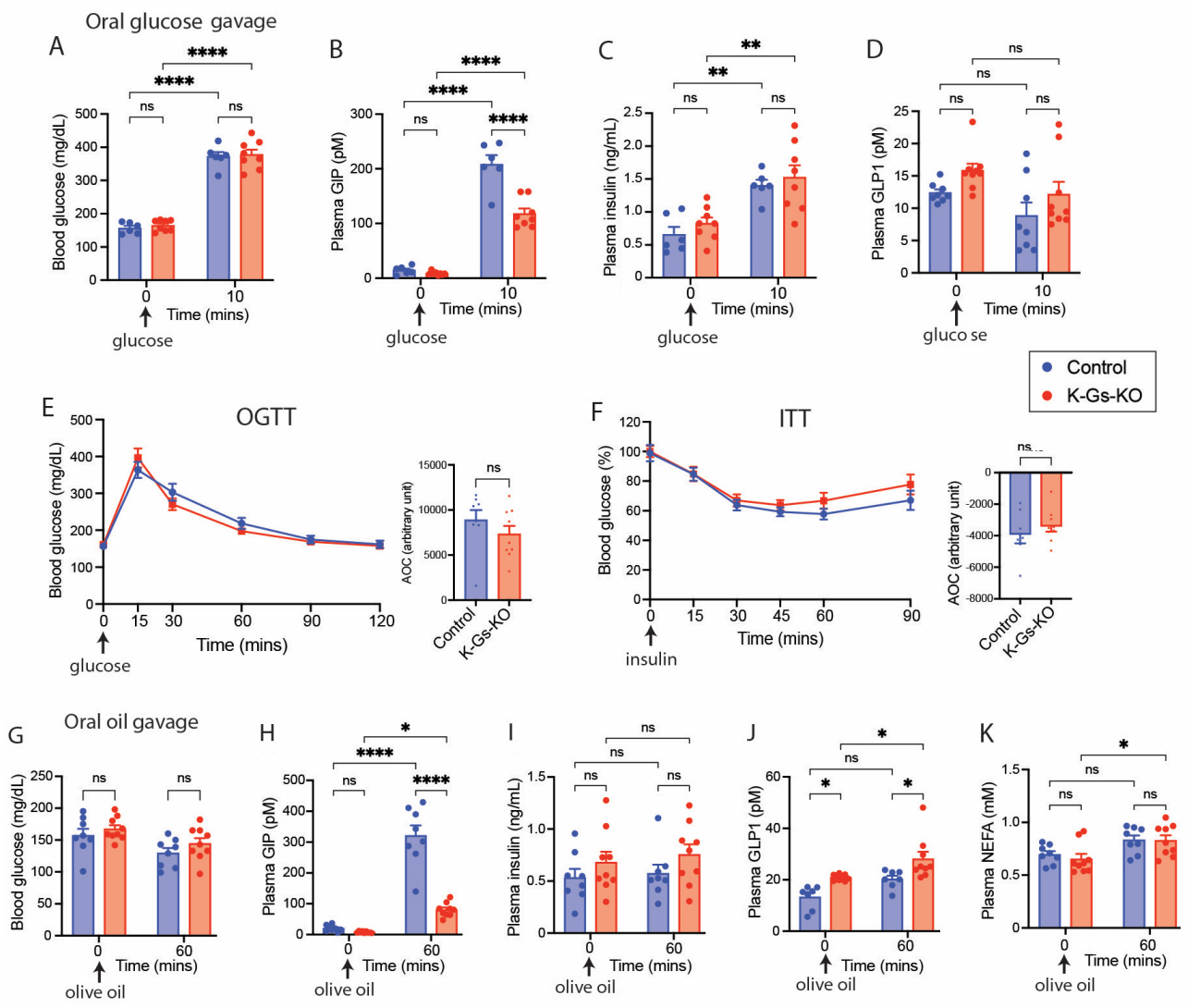

Figure 7. Reduced plasma GIP levels in K-Gs-KO mice do not affect whole-body glucose homeostasis. All studies were carried out with male K-Gs-KO mice and control littermates consuming regular chow. (**A-D**) Blood glucose levels (**A**), and plasma levels of GIP (**B**), insulin (**C**), and GLP1 (**D**), immediately before (time '0') and 10 min after treatment with an oral glucose bolus (2 g/kg). (**E, F**) Oral glucose tolerance test (2 g/kg). (**E**) and insulin tolerance test (0.75 U/kg, i.p.) (**F**). AOC values are shown to the right in each panel. (**G-K**) Blood glucose levels (**G**), and plasma levels of GIP (**H**), insulin (**I**), GLP1 (**J**), and NEFAs (**K**), immediately before (time '0') and 1 hour after oral gavage with olive oil (10 µl/g). All experiments were performed with male mice after a 6-hour fast (the fasting period was only 4 hours for ITT studies). Data are given as means ± SEM (n = 7-10 mice/group). *P<0.05, **P<0.01, ***P<0.001, ****P<0.0001; 2-way ANOVA followed by Tukey post-hoc analysis (**A-D, G-K**) or Student's t-test (**E**, **F**). ns, no statistically significant difference; NEFA, non-esterified fatty acid; AOC, area of the curve.